Available online at www.sciencedirect.com
SCIENCE DIRECT®
Journal of Nuclear Materials 337–339 (2005) 761–765
journal of nuclear materials
www.elsevier.com/locate/jnucmat

Simulation of tokamak armour erosion and plasma contamination at intense transient heat fluxes in ITER

I.S. Landman [a,*], B.N. Bazylev [a], I.E. Garkusha [b], A. Loarte [c], S.E. Pestchanyi [a], V.M. Safronov [d]

[a] *Forschungszentrum Karlsruhe, Institute for Pulsed Power and Microwave Technology, P.O. Box 3640, 76021 Karlsruhe, Germany*
[b] *Institute of Plasma Physics of the National Science Centre, Kharkov Institute of Physics and Technology, Akademicheskaya Street 1, 61108 Kharkov, Ukraine*
[c] *EFDA-Close Support Unit, Garching, Max-Planck Institute für Plasmaphysik, D-85748 Garching bei München, Germany*
[d] *State Research Centre of Russian Federation Troitsk, Institute for Innovation and Fusion Research, 142190 Troitsk, Moscow Region, Russia*

Abstract

For ITER, the potential material damage of plasma facing tungsten-, CFC-, or beryllium components during transient processes such as ELMs or mitigated disruptions are simulated numerically using the MHD code FOREV-2D and the melt motion code MEMOS-1.5D for a heat deposition in the range of 0.5–3 MJ/m^2 on the time scale of 0.1–1 ms. Such loads can cause significant evaporation at the target surface and a contamination of the SOL by the ions of evaporated material. Results are presented on carbon plasma dynamics in toroidal geometry and on radiation fluxes from the SOL carbon ions obtained with FOREV-2D. The validation of MEMOS-1.5D against the plasma gun tokamak simulators MK-200UG and QSPA-Kh50, based on the tungsten melting threshold, is described. Simulations with MEMOS-1.5D for a beryllium first wall that provide important details about the melt motion dynamics and typical features of the damage are reported.

PACS: 52.40.Hf
Keywords: Plasma–material interaction; Erosion; Divertor; ELMs

1. Introduction

In the future tokamak ITER, high heat load transient processes, such as bursts of Edge Localized Modes (ELMs) accompanying normal tokamak operation with a frequency of 1–10^2 Hz, and events of plasma disruptions, are anticipated to present a much more serious problem than in the present-day tokamaks. This is due to ITER's high magnetic field and large plasma volume [1]. The plasma facing components (PFC) of the main chamber wall are to be made of beryllium, and that of the divertor to be carbon fibre composites (CFC) and tungsten (W-brushe). At the divertor, the dome (covered by W-brushe), the limiters, and the top of the vessel, the expected transient heat deposition Q is in the range of 0.5–3 MJ/m^2 on the time scale τ of 0.1–0.5 ms for ELMs and $Q \sim 5$–30 MJ/m^2 at $\tau \sim 1$–10 ms for disruptions [2].

* Corresponding author. Tel.: +49 7247 824696; fax: +49 7247 824874.
E-mail address: igor.landman@ihm.fzk.de (I.S. Landman).

0022-3115/$ - see front matter © 2004 Elsevier B.V. All rights reserved.
doi:10.1016/j.jnucmat.2004.10.083

Such wall load pulses can cause evaporation of a thin layer from the armour surface that after ionization in the impacting plasma stream acts as a plasma shield which expands into the scrape-off layer (SOL).

As the expected fluxes are not achievable in present tokamaks, available non-tokamak facilities must be engaged to simulate such transient loads, for example, with plasma guns that produce streams of hydrogen plasma with Q up to 25 MJ/m^2 and τ up to 0.25 ms [3,4]. This work describes the current state of our theoretical investigations on possible PFC damage, and their correlation with experiments carried out to validate the numerical tools.

So far, the particular loads to different parts of vessel walls are predicted using a scaling which is typical of existing tokamaks [5]. During ELMs the physical carrier of the first wall load is the unstable plasma with electron and ion temperatures $T_e \sim 10$–10^2 eV and $T_i \approx 3$–5 keV, respectively. The hot plasma effectively diffuses across the magnetic surfaces and reaches the target within 0.1 ms after the start of a type I ELM [2]. Assuming that 20–40% of the released energy can arrive at the wall, the load will be in the range of $Q = 0.05$–0.2 MJ/m^2 at τ of 0.2 ms. During a disruption mitigated by impurity puffing (Ne or Ar), the radiation due to the impurity mainly contributes to the first wall load with $Q = 0.5$–1 MJ/m^2 at $\tau \sim 1$ ms [5].

The computational tool applied for a direct calculation of different kinds of transient wall loads is the two-dimensional (2D) multi-fluid MHD code FOREV-2D [6,7] (referred to below as FOREV). It models the irradiation fluxes of the hot plasma lost across the separatrix during an off-normal event and self-consistently calculates the consequent evaporation and ionization of target material, the dynamics of the plasma shield including the radiation transport and its backward propagation. Simulation of plasma dynamics in the ITER geometry with FOREV is described in Section 2.

In the case of metallic targets, the surface damage is substantially caused by melt motion. To model the melting process the incompressible fluid dynamics code MEMOS-1.5D (referred to below as MEMOS) is applied [8]. The tokamak simulators used for validating MEMOS are the plasma guns MK-200UG [3] and QSPA-Kh50 [4]. The validation of MEMOS by these facilities and the surface melting calculations with MEMOS for beryllium armour in ITER are presented (Sections 3 and 4, respectively).

2. Plasma modelling in ITER geometry

The code FOREV was originally developed to describe radiation transport in the dense material plasma near the surface. Therefore it had used a slab geometry and a one-fluid approximation which was sufficient for calculations at plasma densities above 10^{21} m^{-3}. Recently simulations with FOREV also were focused on the ITER ELMy H-mode regime where the vapour shield does not develop or is rather weak compared to the disruption regime. The numerical scheme of FOREV was changed to model the whole SOL, the x-point and inner and outer divertor plates. To distinguish the dynamics of various plasma components, the ion fluids of D, T, He, and C are included. The radiation losses are now taken into account in the approximation of optically thin plasma with the data [9] being the most reliable in this case. However, for the rather dense plasmas of this study this approximation is not correct because the main radiation flux transports in the emission lines where the reabsorption is quite important.

Parametric studies for ELMs were performed so far for the following scenario. It is assumed that the hot DT plasma of the pedestal region is lost during the time $t: 0 < t < \tau$ through the separatrix with a loss rate determined by a specified Q and τ. The plasma then appears in the SOL which has equal constant initial temperatures $T_{DT} = T_e = T_i$ and an exponential density profile, $n_{DT} \propto \exp(-x/d)$, with x the coordinate across SOL and $d \sim 1$ cm the profile thickness. The generated DT plasma heats the carbon-based divertor armour (for the details on the plasma dynamics see Ref. [7]). The values of n_{DT} were varied over the range 2–7×10^{19} m^{-3}, with T_{DT} in the range 1–3 keV, and τ in the range 0.1–0.5 ms. Some results are shown in Fig. 1 for which different points correspond to the regimes with- and without vaporization during the target irradiation. At a regime below the vaporization threshold the surface does not evaporate, because due to a low surface temperature T_s, the vapour saturation pressure is smaller

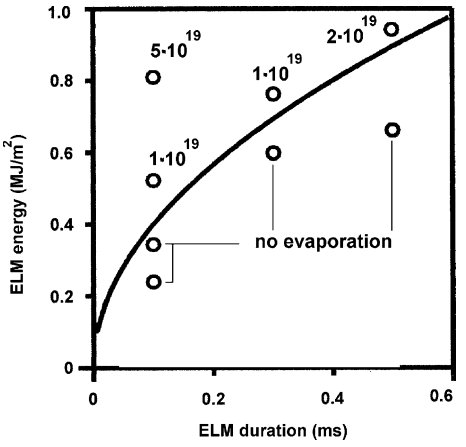

Fig. 1. Evaporation threshold at ITER conditions calculated for carbon-based PFC. The numbers at the points are the maximum carbon density (in m^{-3}) in the SOL obtained for those calculations.

than the impacting plasma pressure. The values of the maximum carbon density (n_c) in the SOL are given for all points above the threshold.

The curve in Fig. 1 presents an analytical solution to the vaporization threshold problem inside the material for a constant impacting heat flux $q = Q/\tau$ which follows from a formula [10] for $T_s(t)$. For $T_s = T_{vap}$ and $t = \tau$: we have $T_{vap} = T_w + 2q/(c\rho)(\tau/\pi\chi)^{1/2}$, with $T_{vap} = 4100$ K the vaporization temperature, $T_w = 1000$ K the initial temperature, c the specific heat capacity, ρ the mass density and χ the heat conductivity of carbon.

To estimate the line radiation transport, the algorithm for plane geometry scenarios available in FOREV with the opacity database TOPATOM [11] is used, assuming that the wall radiation flux is equal to one from the plasma in front of particular wall fragment with the temperature T and the density n of carbon impurity calculated as described above. For the case with $n_{DT} = 3 \times 10^{19}$ m^{-3}, $T = 3$ keV, $\tau = 0.1$ ms and maximum $Q = 0.8$ MJ/m^2 the radiation flux at the vessel walls is shown in Fig. 2 at $t = 15$ ms. The dome and the adjoining divertor parts receive the maximum radiation heat loads. A moderate peak of radiation flux is obtained at the top of the ITER main chamber, due to a decrease of the local poloidal magnetic field and corresponding increase of the SOL thickness. The main contribution comes from a few lines of C^{IV} with photon energies close to 10 eV. However, the line shape is in fact reproduced only by one opacity group, which indicates a poor quality of TOPATOM at the small densities typical for ELMs. These optical data incorporated in FOREV have previously been used at much larger densities typical of the disruption vapour shield. At such large densities the line shape becomes wide enough to describe the powerful lines with several opacity groups.

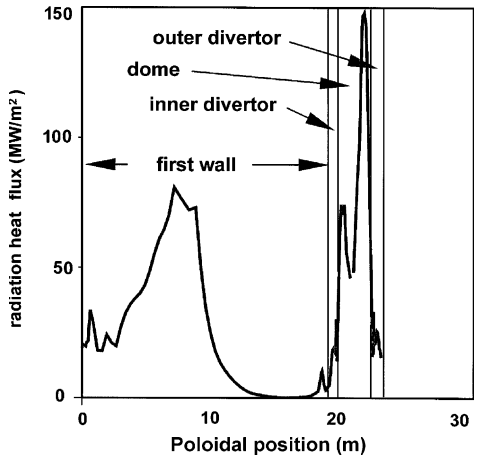

Fig. 2. Radiation load onto ITER vessel walls calculated with FOREV.

3. Melting threshold validation of MEMOS with the plasma guns

Recently the facility MK-200UG was updated for the simulation of heat loads expected at ITER divertor armour for Type I ELMs, and first experiments were performed aimed at the quantification of the tungsten melting threshold. In the experiments, the effective duration of the plasma pulse was of 0.05 ms. The surface temperature T_w was measured with a pyrometer. Fig. 3 demonstrates the time dependence of T_w at the exposed tungsten surface for $Q = 0.28$ MJ/m^2. The dashed curve indicates the tungsten melting temperature $T_{melt} = 3560$ K; T_w is smaller than T_{melt}. At $Q = 0.4$ MJ/m^2, T_w increases rapidly up to T_{melt} but then it remains at this value: evidently the absorbed energy flux is consumed in the melting process. It was concluded that the tungsten melting threshold is ~0.30 MJ/m^2.

A new regime relevant to the ITER ELMs has been found at the facility QSPA-Kh50 also. Calorimetric measurements of Q for multiple (up to 300) pulse irradiations of $\tau = 0.25$ ms are performed, together with observations of melting of micro-hardness markers at the tungsten target, which provided the determination of the melting threshold. After initial exposures the melting threshold was determined as 0.56 MJ/m^2. However, after 150 exposures the melting threshold decreased to 0.45 MJ/m^2, which seems due to material modification and the development of bulk cracks parallel to the target surface that cause decrease of thermal conductivity in a pre-surface layer.

Fig. 3 enables us to assume that the heat pulse at MK-200UG has a sharp front and a long decline, with the shape being somewhere in between that of rectangular- and triangular forms. A similar pulse shape was measured at QSPA-Kh50 with piezoelectric detectors.

For checking these experimental results and guiding MEMOS validation, the tungsten melting threshold was also calculated. In the calculations the triangle

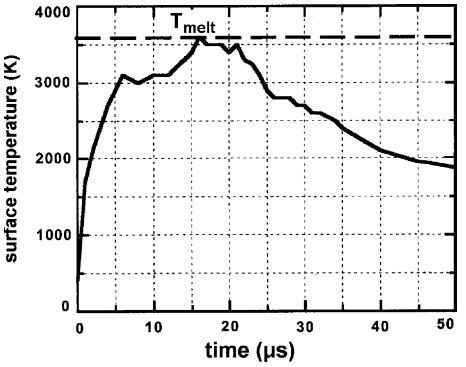

Fig. 3. Surface temperature of a tungsten target obtained at MK-200UG for $Q = 0.28$ MJ/m^2.

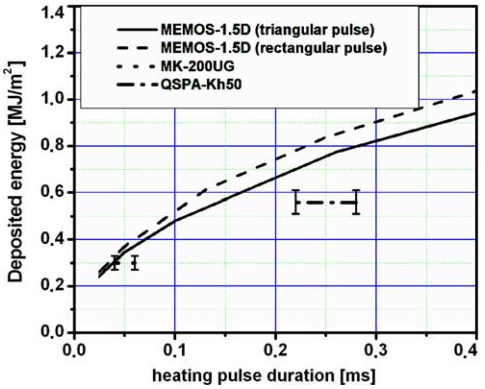

Fig. 4. Comparison of experimental and numerical tungsten melting threshold.

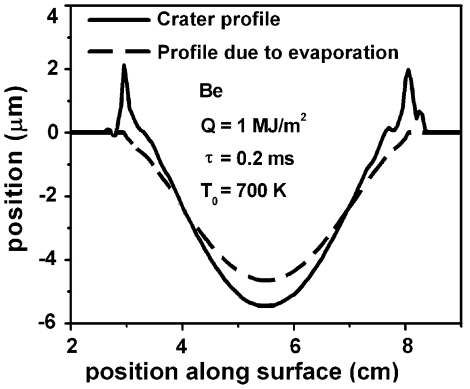

Fig. 5. Beryllium crater profile calculated with MEMOS. The evaporation profile is obtained by stopping the melt motion in the code.

and rectangular shapes of the impinging plasma load in time are assumed, with the pulse durations covering the range 0.05–0.25 ms. Fig. 4 illustrates the experimental results mentioned and the numerical results obtained, with an uncertainty of 15–20% that is caused by the lack of accurate data for tungsten at the temperatures near the melting point. For MK-200UG there is a reasonable agreement, from which it is concluded that the measurements have been carried properly and the validation is successful. The substantial difference of about 30% between QSPA-Kh50 and MEMOS is not yet explained.

4. Surface melting of beryllium armour

Beryllium is foreseen as armour material for the main chamber in ITER. It has been noted that the heat loads during transient events correlate with an electric current of 1–2 MA/m^2 through the armour immersed in strong magnetic field [12]. Here the simulations of beryllium armour damage using the code MEMOS are described. The gradient of surface tension, the Lorentz force of the currents and the gradient of reactive force of evaporated material produce melt acceleration. A two-dimensional heat transport equation describes the temperature inside the target. The Gaussian profile of the heat flux along the surface and the rectangular pulse in time are assumed.

The scenarios relevant to single transient processes are modelled while different heat load parameters are varied: the half-width of the Gaussian profile D from 1 to 50 cm, τ from 0.2 to 1 ms, and the current up to 4 MA/m^2. Vapour shielding was ignored. For the cases with melting, Q was varied from 0.5 MJ/m^2 up to 1 MJ/m^2. The initial target temperature is 700 K. Fig. 5 demonstrates the magnitude of surface roughness obtained in the scenario with obvious evaporation of the melted target at $Q = 1$ MJ/m^2, $\tau = 0.2$ ms and $D = 5$ cm. The maximum elevation of 2 μm and a crater depth of 5.5 μm are obtained. To determine the roles of evaporation and melt motion effects, in one simulation the melt motion was switched off. In this case the crater depth of 4.5 μm was obtained (see Fig. 5); thus the evaporation dominates over the melt motion. In total, the numerical simulations showed that for all scenarios the depth of melt pool ranges between 30 and 55 μm. The melt layer resolidifies after the end of the pulse within 1.5–2.5 ms. A convenient parameter that characterizes the energy pulse is the impact energy $E = Q/\sqrt{\tau}$ as introduced in [13]: At $E < 22$ MJ/(m^2 s$^{1/2}$) a negligible evaporation of the target is obtained. At $E > 25$ MJ/(m^2 s$^{1/2}$) the evaporation becomes dominant. Due to the gradient of the reactive force, the velocity of melt motion at $\tau = 0.2$ ms varies from 0.2 to 0.9 m/s depending on the other parameters, and it exceeds 1 m/s for $\tau = 1$ ms. The surface roughness due to the melt motion reaches 0.5 μm. The Lorenz force intensifies the melt motion. At the current of 2 MA/m^2 the surface roughness reaches 1 μm and the melt velocity increases up to 2–4 m/s.

5. Conclusions

A good correlation between the analytical model and the FOREV comprehensive simulation allows assurance that the vaporization threshold at the target can be estimated using simplified approaches. In the radiation transport calculations for carbon impurities, the line radiation dominates but the data for line shapes need improvements, which demands significant effort for producing new opacities.

Validation of MEMOS against plasma gun experiments at the tungsten melting threshold was successful. The tungsten melting threshold obtained in experiments

on MK-200UG and QSPA-Kh50 is in a reasonable agreement with the calculations of MEMOS, which justifies the application of the code for investigation of melt motion damage at tokamak conditions.

Typical scenarios for transient loads to the beryllium first wall modelled with MEMOS lead to the conclusion that the contribution of evaporation to the damage dominates at the energy impact larger than 25 MJ/(m^2 $s^{1/2}$), with a crater depth of several microns. A rather high melt velocity is obtained when the halo current plays an important role. This can lead to melt splashing and droplet formation.

Acknowledgment

This work has been carried out within the research program of the European Task Force on Plasma–Wall interaction and partially funded by the task TW3-TPP-DISELM of the EFDA technology program.

References

[1] ITER Physics Basics, Nucl. Fus. 39 (1999) 2137.
[2] G. Federici et al., Nucl. Fus. 41 (12R) (2001) 1967.
[3] N.I. Arkhipov et al., J. Nucl. Mater. 233–237 (1996) 767.
[4] V.I. Tereshin et al., J. Nucl. Mater. 313–316 (2003) 686.
[5] A. Loarte et al., these Proceedings. doi:10.1016/j.jnucmat.2004.09.038.
[6] H. Wuerz et al., Fus. Sci. Techn. 40 (2001) 191.
[7] S.E. Pestchanyi, I.S. Landman, H. Würz, Hot plasma contamination in ELMs by divertor material, in: 30th EPS Conference on Contr. Fusion and Plasma Phys., St. Petersburg, 7–11 July 2003, ECA vol. 27A, P-2.164 (CD).
[8] B. Bazylev, H. Wuerz, J. Nucl. Mater. 307–311 (2002) 69.
[9] D.E. Post et al., At. Data Nucl. Data Tables 20 (1977) 397.
[10] L.D. Landau, E.M. Lifshits, Course of Theoretical Physics, vol. 6, Fluid Mechanics, Butterworth-Heinemann, Oxford, 2000.
[11] B. Bazylev et al., Soviet Phys. Eng. J. 58 (1990) 1012 (in Russian).
[12] J. Lingertat et al., J. Nucl. Mater. 241–243 (1997) 402.
[13] A. Hermann et al., J. Nucl. Mater. 313–316 (2003) 759.